MOLECULAR AND CELLULAR BIOLOGY, Dec. 1994, p. 8408–8419
0270-7306/94/$04.00+0

Vol. 14, No. 12

Conjugates of Ubiquitin Cross-Reactive Protein Distribute in a Cytoskeletal Pattern

KEITH R. LOEB AND ARTHUR L. HAAS*

Department of Biochemistry, The Medical College of Wisconsin, Milwaukee, Wisconsin 53226

Received 14 April 1994/Returned for modification 11 July 1994/Accepted 24 August 1994

Ubiquitin cross-reactive protein (UCRP), a 15-kDa interferon-induced protein, is a sequence homolog of ubiquitin that is covalently ligated to intracellular proteins in a parallel enzymatic reaction and is found at low levels within cultured cell lines and human tissues not exposed to interferon. Ubiquitin and UCRP ligation reactions apparently target distinct subsets of intracellular proteins, as judged from differences in the distributions of the respective adducts revealed on immunoblots. In this study, successive passages of the human lung carcinoma line A549 in the presence of neutralizing antibodies against alpha and beta interferons had no effect on the levels of either free or conjugated UCRP, indicating that these UCRP pools are constitutively present within uninduced cells and are thus not a consequence of autoinduction by low levels of secreted alpha/beta interferon. In an effort to identify potential targets for UCRP conjugation, the immunocytochemical distribution of UCRP was examined by using affinity-purified polyclonal antibodies against recombinant polypeptide. UCRP distributes in a punctate cytoskeletal pattern that is resistant to extraction by nonionic detergents (e.g., Triton X-100) in both uninduced and interferon-treated A549 cells. The cytoskeletal pattern colocalizes with the intermediate filament network of epithelial and mesothelial cell lines. Immunoblots of parallel Triton X-100-insoluble cell extracts suggest that the cytoskeletal association largely results from the noncovalent association of UCRP conjugates with the intermediate filaments rather than direct ligation of the polypeptide to structural components of the filaments. A significant increase in the sequestration of UCRP adducts on intermediate filaments accompanies interferon induction. These results suggest that UCRP may serve as a *trans*-acting binding factor directing the association of ligated target proteins to intermediate filaments.

Interferons induce diverse cellular responses contributing to the primary line of defense against viral and parasitic infections and, more generally, modulate the immune system, cell proliferation, and cell differentiation (1, 35). Interferons exert their effects by specifically altering the expression of approximately 30 different intracellular proteins (35). Functions for a few of these interferon-induced proteins have been well characterized and contribute to our understanding of the numerous interferon-mediated effects. However, functions for the majority of these interferon-induced proteins are currently unidentified. The interferon-induced 15-kDa protein, the ISG-15 gene product, belongs to this latter group of proteins. Although it is the predominant alpha/beta interferon (IFN-α/β)-induced protein in Ehrlich ascites tumor cells (3) and is present in extracts of several other interferon-treated cells (6, 16), no functional activity has been attributed to the purified protein. Its temporal expression and concentration dependence on interferon parallel induction of the antiviral response (6). On the basis of these observations, it is assumed that the 15-kDa protein is required in the primary response(s) of cells to interferon.

Recent evidence indicates that the 15-kDa protein is composed of two domains, each of which exhibits significant sequence homology to ubiquitin (6), itself a highly conserved 8.6-kDa protein that participates in a number of fundamental regulatory processes through a unique posttranslational modification in which the carboxyl terminus of the polypeptide is covalently ligated to primary amines on a variety of intracellular proteins (reviewed in reference 9). The amino- and carboxyl-terminal domains of the 15-kDa protein are 43 and 62% homologous to ubiquitin, respectively (6, 19). Symmetry in the positions of homology between the two domains relative to the crystal structure of ubiquitin (41) suggests these two proteins have similar folding motifs (6). The marked sequence similarity of this 15-kDa ubiquitin cross-reactive protein (UCRP) accounts for its initial identification by affinity-purified polyclonal antibodies against ubiquitin (6). Both UCRP and ubiquitin are synthesized as precursors that undergo co- or posttranslational processing to yield identical carboxyl-terminal sequences of Leu-Arg-Leu-Arg-Gly-Gly (15, 31, 34). The resulting exposure of this hexapeptide sequence is functionally significant, since it is the site of isopeptide bond formation to ubiquitin (10) and contributes to interactions with several ubiquitin-specific proteins such as the carboxyl-terminal hydrolases (31) and other enzymes required for target protein conjugation (14, 44). Such similarities led Haas and coworkers to propose that UCRP represents a function-specific homolog of ubiquitin subject to a similar pathway of conjugation within interferon-responsive cells (6). A major consequence of ubiquitin conjugation is the targeting of proteins for degradation via a multienzyme, ATP-dependent degradative pathway (10). Whether UCRP similarly participates in degradative targeting is currently the subject of considerable speculation.

Recently we have exploited immunological methods to confirm the presence of UCRP-protein conjugates within interferon-responsive cells (19, 20). UCRP conjugation apparently differs in target protein specificity from the analogous reaction occurring with ubiquitin. Conjugates to ubiquitin represent a heterogeneous population of adducts, resulting in a diffuse molecular weight distribution on immunoblots probed with antiubiquitin antibodies (7). In contrast, UCRP conju-

* Corresponding author. Mailing address: Department of Biochemistry, The Medical College of Wisconsin, 8701 Watertown Plank Rd., Milwaukee, WI 53226. Phone: (414) 456-8768. Fax: (414) 266-8497.

gates appear as discrete protein bands following immunoblot detection with affinity-purified anti-UCRP antibodies, suggesting a more restricted substrate specificity for formation of such adducts (19). That the pattern of UCRP conjugates is conserved among several cell lines examined indicates similar subpopulations of targets for UCRP ligation (19). Detection of low basal levels of free and conjugated UCRP in cultured cell lines not treated with interferon suggests that UCRP adduct formation may serve a constitutive regulatory function independent of the interferon response. These putative functions are probably similar under constitutive and interferon-responsive conditions, since the intracellular population of these adducts changes in absolute amount but not in distribution upon exposure to the cytokine (19).

One approach to understanding the function of UCRP ligation is the identification and characterization of proteins targeted for conjugation. In this report, we describe immunocytochemical and immunoblot results examining the intracellular distribution of free and conjugated UCRP within cultured human lung carcinoma cells. Our results demonstrate that although most free UCRP exists as a soluble cytosolic protein, a subfraction of immunochemically detected UCRP distributes in a punctate cytoskeletal pattern similar to that observed for intermediate filament-associated proteins. The cytoskeletal distribution is stable to extraction with nonionic detergent and 0.3 M KI, indicating tight association of UCRP with the cytoskeletal network. Immunoblots of parallel detergent-insoluble extracts confirm that the cytoskeletal distribution of UCRP primarily derives from conjugated rather than associated free UCRP.

MATERIALS AND METHODS

Materials. Bovine ubiquitin, bovine gamma globulin, *p*-phenylenediamine, bovine serum albumin (BSA), and protein A were purchased from Sigma. Recombinant UCRP was expressed and purified as previously described (19). Fetal bovine serum and Affi-Gel-10 were obtained from HyClone and Bio-Rad, respectively. Radiolabeled protein A was prepared with Iodogen by using carrier-free $Na^{125}I$ (Amersham Radiochemicals) as described previously (7). Rhodamine phalloidin was from Molecular Probes, Inc. Human recombinant IFN-β_{ser} (10^8 IU/mg) was kindly supplied by Triton Biosciences. Human recombinant consensus$_1$ IFN-α (10^9 IU/mg) was obtained from Amgen Biologicals. Human recombinant keratin 18 was kindly provided by Werner Franke and IIse Hofmann (German Cancer Research Center).

Cell culture and interferon induction. MG-63 (osteosarcoma) and A549 (lung carcinoma) cells were purchased from the American Type Culture Collection and cultured as recommended. Human foreskin cell extracts and primary keratinocytes were generously supplied by George Giudice (Dermatology Department, Medical College of Wisconsin). Cultures were grown at 37°C in a humidified 5% CO_2 atmosphere. The MG-63 and A549 cells were maintained as confluent monolayer cultures in minimal essential medium (Sigma) and Dulbecco's modified Eagle's medium (Sigma), respectively, supplemented with 10% (vol/vol) heat-inactivated fetal bovine serum (HyClone). Keratinocytes were isolated from human foreskin and cultured in Keratinocyte-SFM culture medium (Gibco) as previously described (2). In all experiments, interferon of the indicated type and concentration was added directly to the conditioned culture media 2 days after passage or medium change.

Antibodies. Rabbit anti-UCRP polyclonal antibodies were generated against recombinant mature human UCRP and affinity purified as described previously (19). Rabbit anti-human IFN-β neutralizing antibody was purchased from Lee BioMolecular. Sheep antiserum directed against human leukocyte IFN-α was supplied by Biotech Research (NIAID Repository). Mouse monoclonal anti-β-tubulin antibody (TUB2.1) (23) was purchased from Sigma. Mouse monoclonal antibodies to human keratin 8 (35βH11) and human vimentin (43βE8) (5) were a generous gift from Allen Gown (Department of Pathology, University of Washington). Mouse monoclonal anti-human keratin 18 antibody (CK-5) (39) was obtained from ICN. Rhodamine-conjugated goat anti-mouse immunoglobulin G and fluorescein isothiocyanate (FITC)-conjugated goat anti-rabbit immunoglobulin G antibodies were bought from Cappel.

Solid-phase detection of UCRP. Samples were prepared by rinsing cells in 25 mM potassium phosphate-buffered saline (PBS; pH 7.4) and then subjecting them to lysis in 1× sodium dodecyl sulfate (SDS) sample buffer containing 2% (vol/vol) β-mercaptoethanol (6). The resulting extracts were briefly sonicated for 10 s, boiled for 2 min, and resolved by SDS-polyacrylamide gel electrophoresis (PAGE) on a 12% (wt/vol) polyacrylamide gel before electrophoretic transfer to Schleicher & Schuell BA83 nitrocellulose membranes (7). Blots were immunostained with 10 μg of affinity-purified anti-UCRP antibody per ml in Tris-saline (50 mM Tris-Cl [pH 7.4], 150 mM NaCl) containing 25 mg of BSA per ml and visualized by autoradiography after incubation with ^{125}I-protein A (7, 19).

Immunocytochemical localization of UCRP. Subconfluent cultures of A549, MG-63, or primary keratinocytes were grown on glass coverslips and incubated in the presence or absence of 1,000 IU of IFN-β per ml for 24 h. Fixed whole cells were prepared by ethanol (EtOH)-ether treatment (42); briefly, cells were rinsed in PBS and then fixed by successive incubations in 70% EtOH (15 min), 50% EtOH–50% ether (30 min), 70% EtOH (3 min), 50% EtOH (15 min), and H_2O (15 min). Fixed cells were again rinsed five times in PBS to remove trace organic solvents and stored overnight in the same buffer.

Other samples were progressively extracted with Triton X-100, using a modified version of the method of Heuser and Kirschner (11), prior to fixation for 30 min at 37°C in 4% paraformaldehyde freshly prepared in stabilizing buffer [100 mM piperazine-*N*,*N*′-bis(2-ethanesulfonic acid) (PIPES; pH 6.9), 0.5 mM $MgCl_2$, 0.1 mM EDTA] (8). Cells were rinsed twice in PBS at 37°C prior to differential extraction. Under conditions of extraction 1, designed to preserve all cytoskeletal elements, cells were incubated 3 min (37°C) in stabilizing buffer containing 0.5% Triton X-100 and 4 M glycerol prior to fixation. The conditions of extraction 2, which retain the actin and intermediate filaments while quantitatively solubilizing the tubulin network, required incubation for 30 min (37°C) in stabilizing buffer containing 0.5% Triton X-100 in the absence of glycerol. The most stringent procedure, extraction 3, was designed to remove both tubulin and actin networks while retaining intact intermediate filaments and required incubation for 30 min (37°C) with 0.5% Triton X-100 in stabilizing buffer followed by a 3-h incubation in the presence of 0.3 M KI at 4°C. For all three extraction protocols, the cells were rinsed five times in PBS following fixation.

Fixed monolayers were initially incubated in blocking solution (50 mM Tris-Cl [pH 7.6], 150 mM NaCl, 25 mg of BSA per ml) to eliminate nonspecific binding and then incubated for 1 h with 10 μg of either affinity-purified anti-UCRP or antiubiquitin antibody per ml diluted in the same solution (8). The concentration of primary antibody used in these experiments was determined from independent range studies. The cells were then rinsed three times for 10 min each time with Tris-

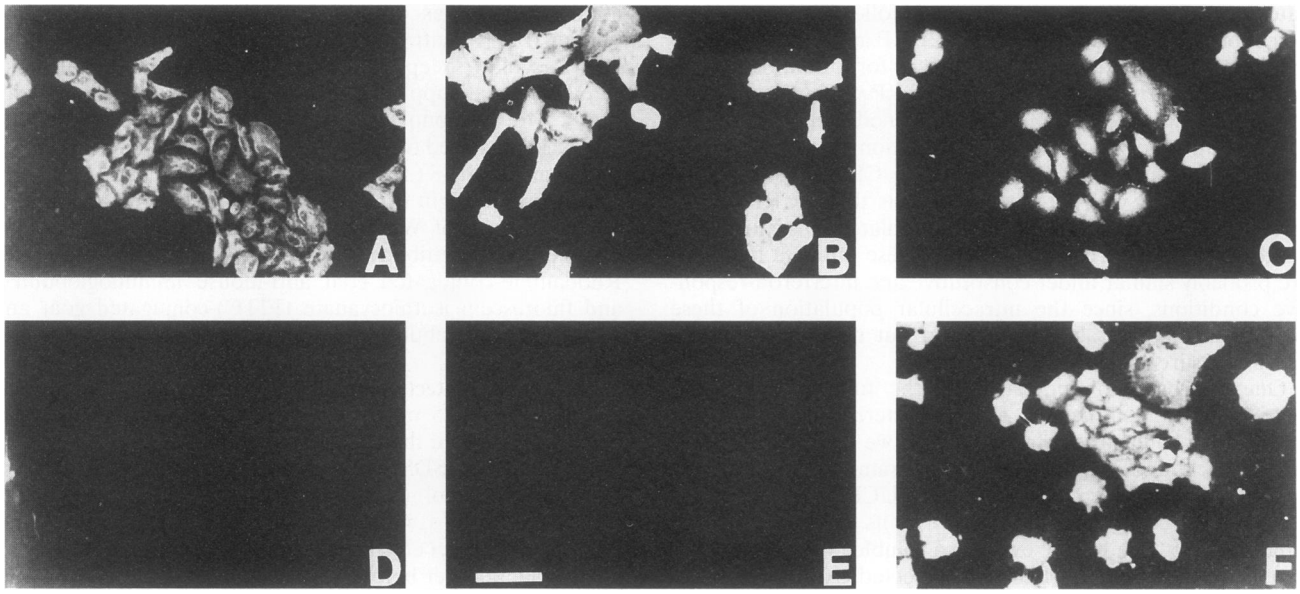

FIG. 1. Immunocytochemical detection of UCRP in A549 cells. Subconfluent A549 cells grown on glass coverslips were rinsed three times with PBS and prepared by EtOH-ether fixation (42). The fixed cells were then stained with the indicated primary antibody at 10 μg/ml in blocking solution followed by FITC-conjugated goat anti-rabbit antibody diluted 1:100 in blocking solution. (A) Control A549 cells stained with anti-UCRP antibody; (B) A549 cells treated for 24 h with 1,000 IU IFN-β_{ser} per ml and then stained with anti-UCRP antibody; (C) control A549 cells identical to those in panel A but stained with antiubiquitin antibody; (D) control A549 cells identical to those in panel A but stained with FITC-conjugated goat anti-rabbit antibody in the absence of any primary antibody; (E) IFN-β-treated A549 cells identical to those in panel B but stained with anti-UCRP antibody that had been preincubated with a 200-fold mole excess of free recombinant UCRP; (F) IFN-β-treated A549 cells identical to those in panel B but stained with anti-UCRP antibody that had been preincubated with a 200-fold mole excess of free ubiquitin. All panels have been exposure normalized. Bar = 20 μm.

saline and stained for 1 h with FITC-conjugated goat anti-rabbit antibodies (1:100 dilution in blocking solution). The titer of the secondary antibody was empirically determined to minimize both nonspecific staining in the absence of the primary antibody and signal crossover with the complementary barrier filter when double-antibody colocalization procedures were used. The coverslips were rinsed three times with Tris-saline and then inverted and mounted on glass slides, using a glycine buffer containing *p*-phenylenediamine (0.1%) antiquenching agent (13). For colocalization studies, incubation with anti-UCRP as the first primary antibody was followed by incubation with FITC-conjugated goat anti-rabbit antibodies. The cells were stained with the indicated monoclonal antibody and then incubated with rhodamine-conjugated goat anti-mouse antibodies. Actin filaments were detected with rhodamine-conjugated phalloidin diluted in blocking solution. Slides were viewed on a Nikon Optiphot epifluorescence microscope. The FITC filter was a blue filter with absorbance maximum at 495 nm, while the rhodamine filter was a green filter with absorbance maximum at 546 nm.

RESULTS

Immunocytological localization of UCRP in cultured A549 cells. Immunocytological localization of UCRP within the A549 human cell line was examined as a potential means of identifying intracellular proteins targeted for ligation. Subconfluent cultures of A549 cells grown on glass coverslips were treated for 24 h with 1,000 IU of IFN-β per ml and then fixed by the EtOH-ether procedure (42) described in Materials and Methods. Fixed cells were stained with affinity-purified anti-UCRP antibodies at a concentration of 10 μg/ml. The intracellular distribution of UCRP was monitored by indirect immunofluorescence microscopy using FITC-conjugated goat anti-rabbit secondary antibodies. As shown in Fig. 1A, a low constitutive level of UCRP was immunocytochemically detected in the absence of interferon treatment. The staining pattern in uninduced cells revealed a characteristic perinuclear distribution and cytoplasmic network closely resembling that reported for cytoskeletal proteins. Induction of UCRP by 24-h treatment with IFN-β produced an intense but diffuse staining pattern throughout the entire cell, presumably due to increases in the levels of free and conjugated UCRP (Fig. 1B). Although not apparent in the exposure normalized micrograph of Fig. 1, a discernible filamentous pattern of UCRP deposition continued to be visible against the diffuse staining background for IFN-β-induced cells (see Fig. 2). No staining was visible when IFN-β-treated A549 cells were incubated with only the FITC-conjugated goat anti-rabbit secondary antibody, demonstrating lack of cross-reactivity with human A549 cells (Fig. 1D).

Specificity of the immunostaining for UCRP was suggested by the observation that affinity-purified anti-UCRP antibodies used at concentrations ranging from 0.5 to 10 μg/ml generated similar staining patterns differing only in signal intensity (not shown). Additionally, affinity-purified anti-UCRP antibodies isolated from three different rabbits generated similar staining patterns in EtOH-ether-fixed A549 cells (not shown). Previous studies have proposed that ubiquitin also distributes in a fibrous network (22, 29, 30). Three lines of evidence indicate that the filamentous pattern observed with anti-UCRP antibody does not result from cross-reaction with ubiquitin: (i) the anti-UCRP antibody does not recognize either free or conjugated ubiquitin when used to probe immunoblots (19); (ii) immunocytochemical staining of untreated A549 cells with antiubiquitin antibodies revealed a diffuse cytoplasmic staining with an intense nuclear distribution (Fig. 1C) that was dis-

tinctly different from that observed with the anti-UCRP antibody (Fig. 1A), even at high magnification (not shown); and (iii) the immunospecific signal observed with anti-UCRP antibody was quantitatively blocked by preincubation with a 200-fold mole excess of free recombinant UCRP but not by an equivalent amount of ubiquitin (Fig. 1E and F, respectively).

UCRP distributes in a punctate cytoskeletal pattern. The panels in Fig. 1 were photographed at higher magnification to illustrate more clearly the fibrous pattern of UCRP and potential changes following IFN-β treatment. In the absence of interferon treatment, UCRP displayed a predominantly cytoplasmic fibrous distribution with a perinuclear pattern that became more punctate toward the cell periphery (Fig. 2A). Interferon treatment markedly elevated the level of immunospecific UCRP signal, as seen by the brighter staining in Fig. 2B, which was exposed under the same conditions as Fig. 2A to allow direct comparison. However, a shorter exposure of the field in Fig. 2B demonstrated that UCRP was still organized in a predominantly fibrous pattern identical to that observed in uninduced cells (Fig. 2C).

In previous studies, we have shown that the anti-UCRP antibody does not discriminate between free and conjugated polypeptide present on immunoblots (19); therefore, it is not possible to distinguish whether the distribution observed in Fig. 2 results from free, conjugated, or both forms of UCRP. Since 60 to 80% of total UCRP is found ligated to target proteins within A549 cells (19), it is likely that the immunocytological signal present in Fig. 2 represents conjugated polypeptide. The kinetics of UCRP induction following exposure to interferon show a characteristic pattern in which there is an initial increase in the level of free UCRP during the first 12 h of interferon exposure followed by an elevation of UCRP conjugates during the subsequent 12 h as the free pool undergoes ligation (19). We exploited this differential induction to examine possible redistribution of signal under conditions for which either free or conjugated polypeptide dominated. An experiment identical to that of Fig. 2 was performed following incubation of A549 cells with IFN-β for either 12 or 24 h. The majority of the increased UCRP signal in cells treated for 12 h with IFN-β resulted from a diffuse staining pattern whose overall localization remained unchanged as UCRP was subsequently conjugated to substrate proteins during the next 12 h (not shown). Although no significant differences in immunocytochemical localization could be detected between cells containing a large percentage of free UCRP (12 h of interferon treatment) versus those containing mostly conjugated UCRP (24 h of interferon treatment), the cytoskeletal distribution of UCRP staining remained relatively unchanged. In agreement with previous immunoblot analyses (19), these results suggest that the substrate proteins for UCRP conjugation and their intracellular distribution remain constant following interferon treatment.

UCRP is present constitutively in A549 cells. As shown above, the intracellular distribution of anti-UCRP reactive proteins in cells exposed to interferon is considerably more complex than that from untreated cells. Furthermore, the fraction of conjugated UCRP in A549 cells relative to that of the free form is greatest before interferon treatment (19). For these reasons, we chose to focus on the distribution of UCRP conjugates under constitutive conditions for which the immunocytochemical analysis would best reflect the distribution of UCRP conjugates rather than free cytoplasmic UCRP.

Low constitutive levels of both UCRP mRNA and protein have been detected in a number of cultured cell lines and human tissue in the absence of interferon treatment (3, 6, 19, 20, 32). However, the presence of UCRP in uninduced cells could be due to a constitutive role for the protein or could result from autoinduction by low levels of secreted IFN-α/β. To resolve this question prior to further immunolocalization studies, confluent cultures of A549 cells were passaged three times in the presence of neutralizing antibodies against both human IFN-α and IFN-β. Cultures were then grown for an additional 24 h in the absence or presence of various doses of either IFN-α or IFN-β to verify the neutralizing activity of the

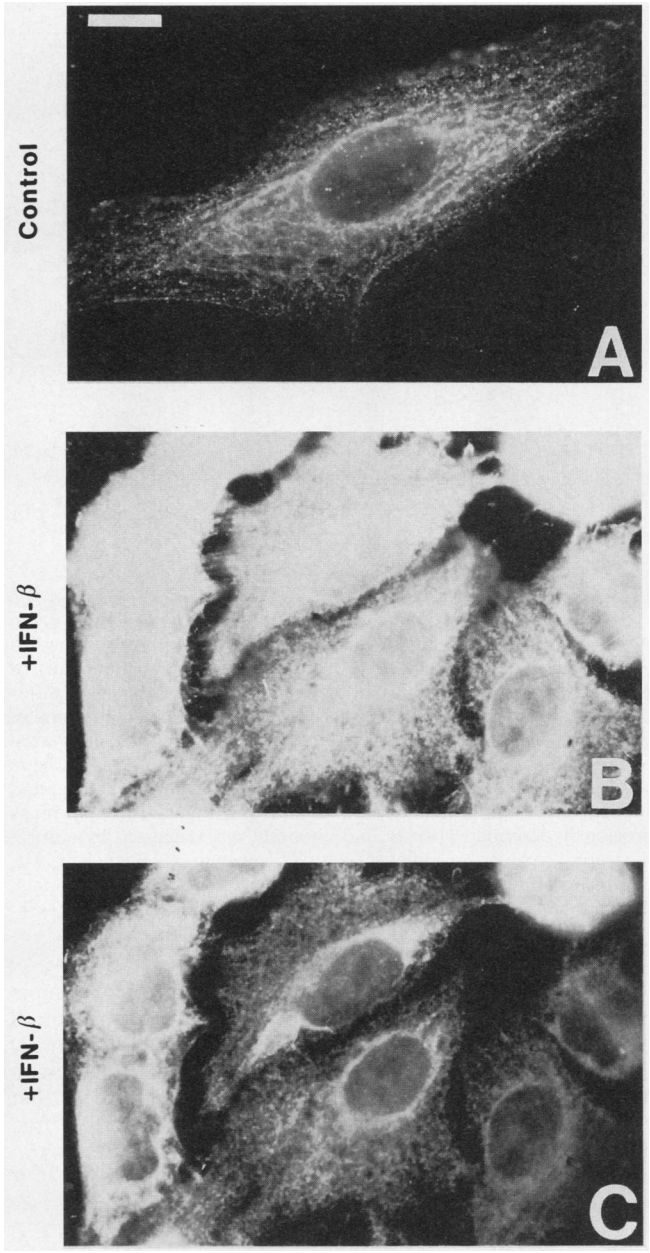

FIG. 2. Intracellular distribution of UCRP in A549 cells. Subconfluent A549 cells grown on glass coverslips were incubated for 24 h in the absence (A) or presence (B and C) of 1,000 IU of IFN-β per ml. Cells were then fixed and stained with anti-UCRP antibody as described in the legend to Fig. 1. Panels A and B were made at identical exposures to demonstrate the increase in immunospecific UCRP signal following interferon treatment. Panel C is a fivefold-shorter exposure of panel B to illustrate better the continued fibrous distribution of UCRP following interferon stimulation. Bar = 4 μm.

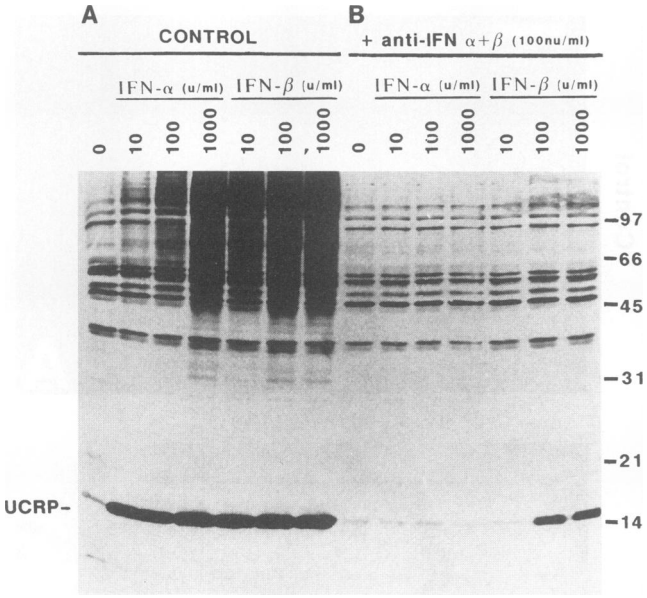

FIG. 3. Free and conjugated forms of UCRP exist constitutively in A549 Cells. Confluent monolayer cultures of A549 cells were grown in the absence (A) or presence (B) of 100 neutralizing units (nu) of neutralizing antibodies against both human IFN-α and -β per ml. After three passages, the cells were induced with the indicated amounts of human recombinant IFN-α or -β_{ser} for 24 h. Thereafter, cells were lysed by the addition of SDS sample buffer, and then proteins were resolved by SDS-PAGE (12% gel), transferred to nitrocellulose, and stained with 10 μg of affinity-purified anti-UCRP antibodies per ml as previously described (19). Bound antibody was visualized by autoradiography following incubation with ^{125}I-protein A. Each lane was loaded with 8×10^4 cells. The mobilities of UCRP and molecular mass markers (in kilodaltons) are indicated at the left and right, respectively.

antibodies. Cultured cells were lysed directly into SDS sample buffer, resolved by SDS-PAGE (12% gel), and electroblotted onto nitrocellulose (BA83; Schleicher & Schuell) as previously described (19). The resulting immunoblots were probed with affinity-purified rabbit polyclonal anti-UCRP antibodies that recognize neither free nor conjugated ubiquitin. Levels of free and conjugated UCRP were then visualized by autoradiography, after which the immunoblot was incubated with ^{125}I-protein A (19).

The results of a representative experiment are shown in Fig. 3. Figure 3A illustrates the induction of free and conjugated UCRP in response to increasing amounts of IFN-α or IFN-β for cultures passaged in the absence of neutralizing antibodies. Both interferons induced the synthesis of free UCRP at low doses and the accumulation of UCRP conjugates at higher doses (19), as noted in Fig. 3 for IFN-α. Concentrations of IFN-β below 10 U/ml are required to observe similar differential induction (19). Previous work (19) and shorter exposures of Fig. 3 (not shown) reveal that although the qualitative distribution of UCRP conjugates is conserved in cells treated with different amounts of IFN-α or -β, some UCRP adducts appear to be induced by interferon treatment while others remain unchanged from the levels present in the absence of induction. Figure 3B shows parallel samples from cultures passaged in the presence of 100 neutralizing units each of anti-IFN-α and -β per ml. The neutralizing antibodies eliminated the induction of UCRP by 1,000 IU of IFN-α and 10 IU of IFN-β per ml. Neutralizing antibodies against IFN-β were not adequate to block induction of free UCRP above 100 IU of IFN-β per ml but did significantly attenuate the subsequent accumulation of UCRP conjugates that occurs at higher concentrations of the cytokine (19). Most significantly, similar low levels of both free and conjugated UCRP were present in control cells passaged either in the absence or in the presence of the neutralizing antibodies (lanes O). The latter observation confirms that both free and conjugated forms of UCRP are constitutively present in A549 under conditions in which autoinduction is precluded.

The filamentous distribution of UCRP does not associate with microtubules or actin fibers. It has been reported that free ubiquitin colocalizes with both microtubules and nuclear spindles (29). To determine if the filamentous distribution of UCRP observed in Fig. 1 and 2 resulted from constitutive association of the polypeptide with these fibers or other cytoskeletal components, A549 cells were progressively extracted by the procedure of Heuser and Kirschner (11) as described below and in Materials and Methods. This extraction protocol exploits the differential solubility of the various cytoskeletal components.

Untreated A549 cells were sequentially extracted with 0.1% Triton X-100 in stabilizing buffer in the presence (extraction 1) or absence (extraction 2) of 4 M glycerol or in the absence of glycerol and then with 0.3 M KI (extraction 3) prior to fixation with paraformaldehyde. These extractions are reported to preserve the tubulin, actin, and intermediate filament networks (extraction 1), to extract the tubulin network while preserving the actin and intermediate filaments (extraction 2), or to extract all cytoskeletal structures except for the intermediate filament network (extraction 3) (11). After fixation, the coverslips were stained with rabbit anti-UCRP antibodies and TUB2.1, a monoclonal antibody directed against β-tubulin (23). Immunospecifically bound antibodies were detected with either FITC-conjugated goat anti-rabbit antibody (anti-UCRP) or rhodamine-conjugated goat anti-mouse antibody directed against TUB2.1 (Fig. 4). Under these conditions, there was no detection of the rhodamine signal when viewed through the FITC filter or of the FITC signal when viewed through the rhodamine filter (data not shown). Separate control experiments also demonstrated that there was no cross-reaction of secondary antibodies with the fixed cellular proteins or cross-species recognition of the inappropriate primary antibody, since no signal was observed when the appropriate primary antibody was excluded (data not shown).

The least rigorous extraction (extraction 1) left a well-defined tubulin pattern that bears no resemblance to the punctate fibrous pattern found with affinity-purified anti-UCRP antibodies (Fig. 4A and B). The tubulin network began to collapse under the conditions of extraction 2, since the microtubules began to retract from the cell periphery and acquired a punctate appearance at their distal ends (Fig. 4D). The pattern obtained with anti-UCRP following extraction 2 did not resemble the pattern for tubulin (Fig. 4C). Under the most rigorous conditions of extraction 3, the tubulin staining was quantitatively eliminated while that of UCRP was retained (Fig. 4E and F). The organization of UCRP was slightly altered by extraction 3 such that the punctate pattern appeared to condense into a more tightly packed network.

The absence of colocalization between the fibrous pattern of UCRP and the tubulin network was confirmed by three additional observations. (i) Double exposures of these extracted cells showed that the UCRP signal did not coincide with that of tubulin (data not shown). A few areas stained with both antibodies; however, this appeared to result from intersecting fibers rather than the distribution of UCRP reactive proteins along the microtubules. (ii) The tubulin network was

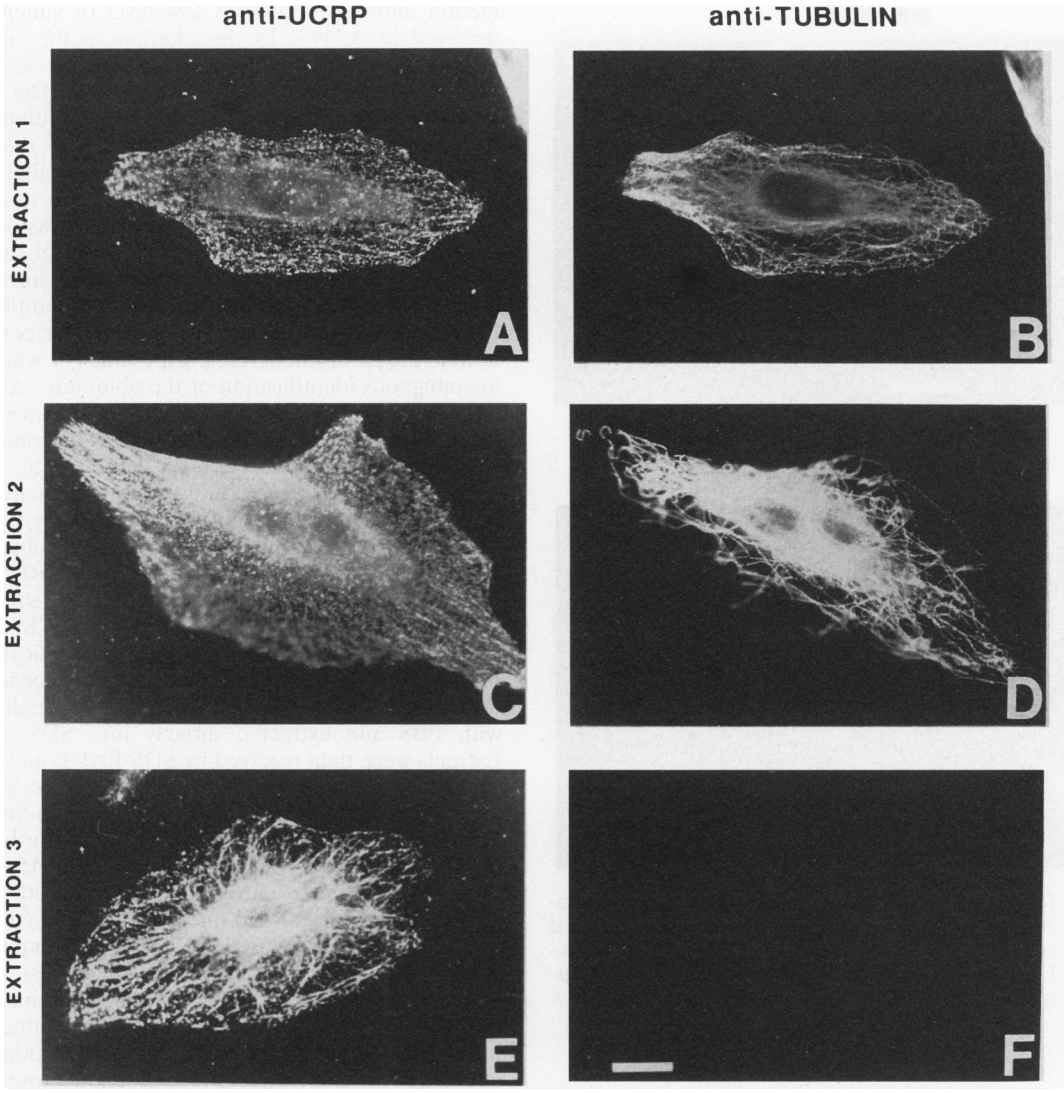

FIG. 4. UCRP does not distribute along the tubulin network. Subconfluent cultures of A549 cells were grown on glass coverslips and were extracted as described in Material and Methods: (A and B) 0.5% Triton X-100 and 4 M glycerol for 3 min at 37°C; (C and D) 0.5% Triton X-100 for 30 min at 37°C; (E and F) 0.5% Triton X-100 for 30 min at 37°C followed by 0.3 M KI at 4°C (11). Following extraction, the cell lysates were fixed with 4% paraformaldehyde for 30 min at 37°C (8). Subsequently, the cells were stained with rabbit anti-UCRP antibody and detected with FITC-conjugated goat anti-rabbit antibody and then stained with mouse anti-β-tubulin antibody (TUB2.1) and detected with rhodamine-conjugated goat anti-mouse antibody. (A, C, and E) FITC filter; (B, D, and F) rhodamine filter. Bar = 4 μm.

not stable to the EtOH-ether fixation technique originally used to identify the UCRP fibrous pattern, indicating that the fibrous pattern observed with anti-UCRP probably did not result from an association with the tubulin network. (iii) In one optical field, we observed two cells undergoing mitosis in which the spindles stained intensely with the antitubulin antibody; however, there was no recognition of these structures by the anti-UCRP antibody (Fig. 5).

A similar study was performed to determine if UCRP localized with the actin microfilaments. In these studies, rhodamine-conjugated phalloidin was used to detect actin filaments. Phalloidin preferentially binds filamentous actin to the exclusion of the free monomer, obviating background detection of the latter (38). Some degree of colocalization was detected in the cell periphery and extracellular attachment sites, which stained brightly when probed with phalloidin and anti-UCRP antibodies (not shown). However, many of the punctate filaments of UCRP were not detected by phalloidin, and the progressively rigorous extractions eliminated all recognition by phalloidin, suggesting that much of the UCRP pattern was not associated with the actin filaments.

UCRP distributes along the keratin filaments. The ability of the UCRP staining to resist extraction with both nonionic detergents and high concentrations of KI suggested that UCRP may be tightly associated with the intermediate filament network that is also highly resistant to these extractions. Association of UCRP with intermediate filaments was confirmed in EtOH-ether-fixed A549 cells by immunocytochemical colocalization of UCRP with cytokeratin, a constituent of these structures (Fig. 6A and B). Cytokeratin 8 was stained with monoclonal antibody 35βH11 (5) and detected with rhodamine-conjugated goat anti-mouse antibodies. Figure 6 also compares the staining of UCRP in A549 cells with that of cytokeratin 8 as a function of different extraction protocols.

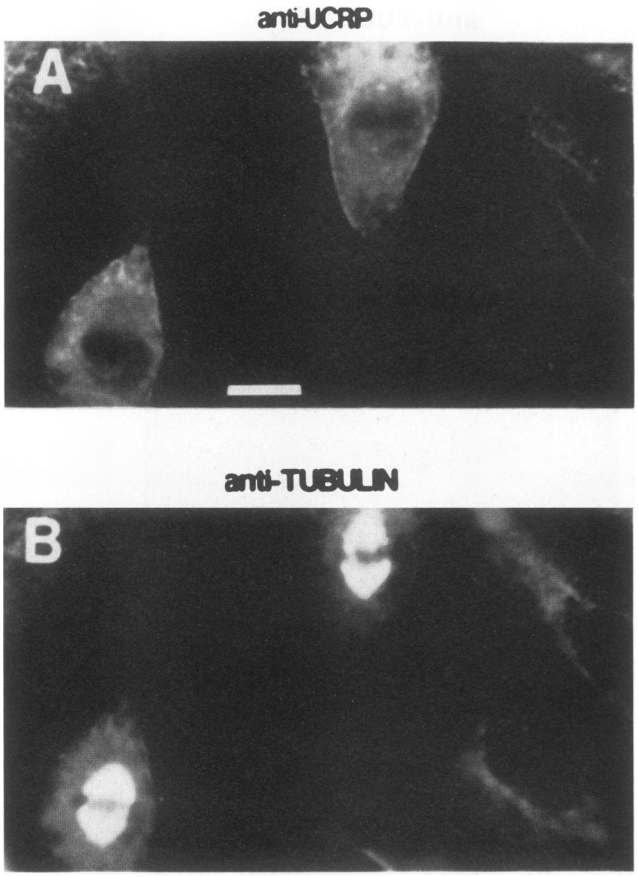

FIG. 5. UCRP does not associate with mitotic spindles. Subconfluent cultures of A549 cells were grown on glass coverslips and prepared by using extraction 1 (Material and Methods). The cells were subsequently stained first with anti-UCRP antibody and then with anti-β-tubulin antibody (TUB2.1) as described in the legend to Fig. 4. Bar = 4 μm.

Under the most rigorous conditions of extraction 3, the patterns of UCRP staining closely colocalized with the cytokeratin network, which appeared as a complex collection of interdigitating fibers forming a perinuclear pattern that extended toward the periphery (Fig. 6G and H). Double exposures of parallel experiments showed that not all areas of the cytokeratin network contained a detectable UCRP signal. These regions with unassociated UCRP appeared to be randomly distributed throughout the keratin network (data not shown).

To determine if the intermediate filament association of UCRP was specific for cytokeratin, the human osteosarcoma cell line MG-63, which expresses vimentin rather than keratin, was also examined (not shown). A similar pattern of punctate fibers that was highly resistant to extraction with nonionic detergent was observed in MG-63 cells stained with anti-UCRP. No signal was detected when cells were stained with either 35βH11 or CK-5, a monoclonal antibody specific for cytokeratin 8 or 18, respectively (5, 39). However, 43βE8, a monoclonal antibody directed against vimentin (5), stained the intermediate filament network and also colocalized with the punctate fibrous pattern characteristic of anti-UCRP staining. In contrast to results with the A549 cells, some of the UCRP filamentous signal present in MG-63 cells stained independent of the intermediate filament networks revealed by the antivimentin antibody 43βE8. A low level of vimentin fibers was detected in A549 cells, in addition to the signal from the keratin network, which also showed an association with UCRP-immunospecific signal (not shown). The latter observations indicate that anti-UCRP detects a population of proteins that associate in a punctate pattern with the intermediate filament network of cells derived from mesothelial and epithelial origins. Finally, UCRP was also shown to distribute in a qualitatively similar intermediate filament-associated pattern within cultures of primary keratinocytes (not shown).

UCRP conjugates are associated with intermediate filaments. The affinity-purified antiubiquitin antibody used for Fig. 1 exhibits a documented specificity for conjugated ubiquitin to the exclusion of free polypeptide (7), which provides an unambiguous identification of the ubiquitin adducts in immunocytochemical applications (33). In contrast, the affinity-purified anti-UCRP antibodies do not discriminate between free and conjugated UCRP (19); therefore, the immunolocalization of UCRP signal to intermediate filaments could potentially arise through binding of the free polypeptide to these fibers, as apparently occurs between free ubiquitin and the cytoskeleton (4, 29), or by association of UCRP conjugates. To distinguish between these two possibilities, subconfluent cultures of A549 cells were grown on coverslips in the absence or presence of IFN-β under conditions identical to those for preparation of samples for the immunocytochemical studies described earlier. Cells contained on the coverslips were rinsed with PBS and extracted directly into SDS sample buffer. Extracts were then resolved by SDS-PAGE and either stained directly with Coomassie blue (Fig. 7) or electroblotted onto nitrocellulose and probed with anti-UCRP antibodies (Fig. 8).

IFN-β treatment had a negligible effect on both the distribution and amount of total protein in A549 cells, since qualitatively similar patterns were observed in whole cell samples from control and interferon-treated cultures (Fig. 7). The organic fixation used for the initial immunocytological studies shown in Fig. 1 and 2, which best preserved the filamentous pattern of UCRP, retained the majority of these cellular proteins (Fig. 7, EtOH/Ether). In contrast, most of the intracellular proteins in both untreated and induced cells were eliminated by the progressive extraction protocol. The most rigorous extraction in the presence of 0.3 M KI (Fig. 7, Ext.3) eliminated almost all of the cytoskeletal proteins in the range of 40 to 70 kDa that had been retained by extraction 2, leaving only the highly insoluble subunits of the intermediate filaments and four low-molecular-mass (<20-kDa) intermediate filament-associated proteins. The prominent 57-kDa band retained in extract 3 was identified as vimentin on a parallel immunoblot stained with the 43βE8 monoclonal antibody specific for this isoform (not shown). Extract 3 also contained less abundant bands of 45 kDa (cytokeratin 18) and 52.5 kDa (cytokeratin 8) that were identified by immunoblotting with the specific CK-5 and 35βH11 monoclonal antibodies, respectively (not shown).

Figure 8 shows the pattern of anti-UCRP-immunoreactive proteins contained in A549 samples from a Western blotting (immunoblotting) analysis performed in parallel to the experiment represented by the gel shown in Fig. 7. There is a marked induction of UCRP following IFN-β treatment in whole cell extracts. Approximately 70% of total UCRP was present in conjugated form within untreated cells (Fig. 8A, Whole Cell Control), as judged from quantitation of free and adduct pools within this sample as described previously (19). Interferon treatment increased the absolute amounts of free and conjugated UCRP disproportionately, leading to a decrease in the level of conjugated UCRP to 60% of the total polypeptide

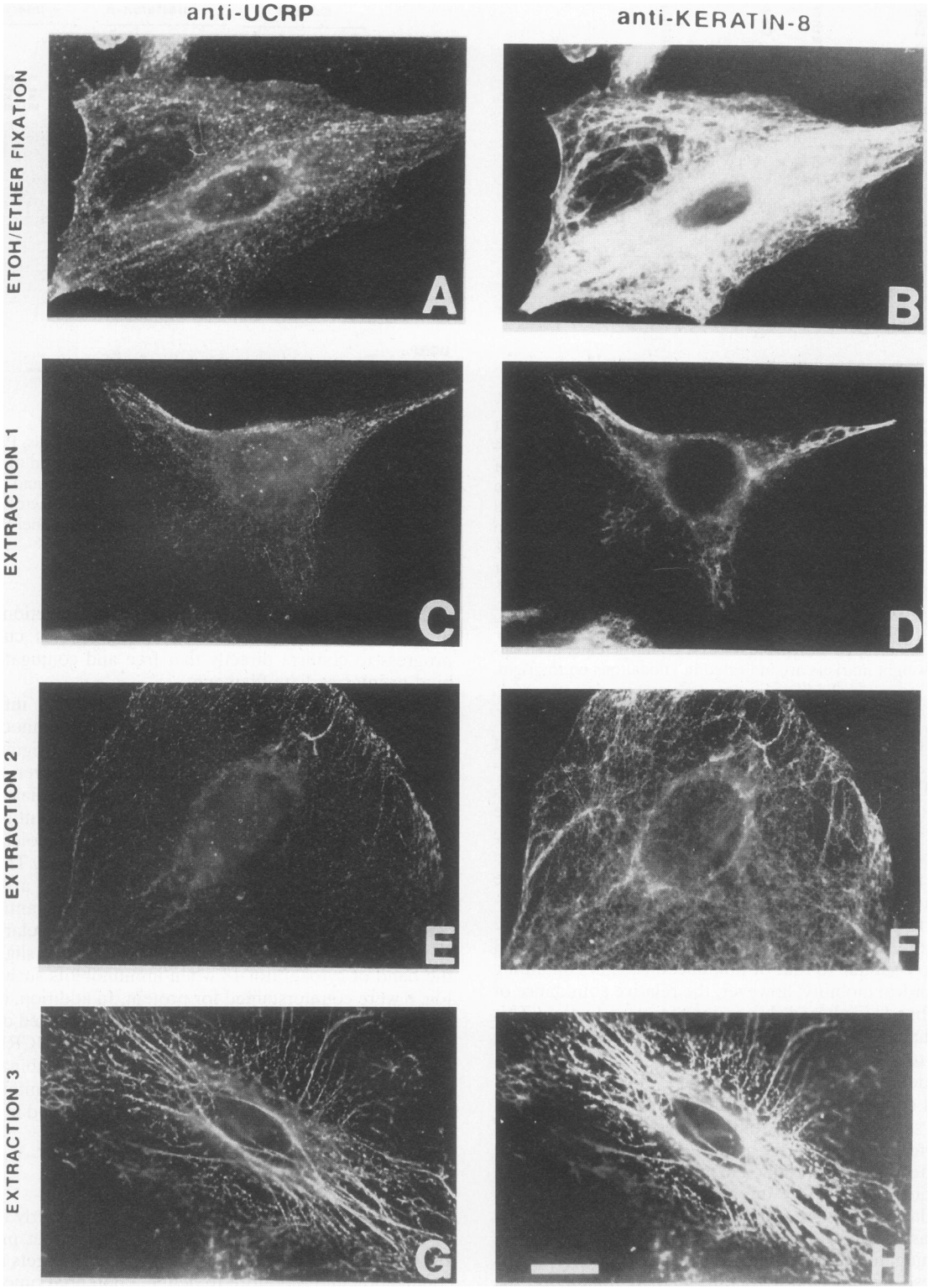

FIG. 6. UCRP distributes along the keratin network. Subconfluent cultures of A549 cells were fixed with successive incubations in 70% EtOH for 15 min, 50% EtOH–50% ether for 30 min, 50% EtOH for 15 min, and 100% H_2O for 15 min (A and B) (42). Cells were also extracted as described in Materials and Methods with 0.5% Triton X-100 and 4 M glycerol for 3 min at 37°C (C and D), 0.5% Triton X-100 for 30 min at 37°C (E and F), and 0.5% Triton X-100 for 30 min at 37°C and then 0.3 M KI at 4°C (G and H) (11). Following extraction, the cells were fixed with 4% paraformaldehyde for 30 min at 37°C (8). The cells were initially stained with anti-UCRP antibody and detected with FITC-conjugated goat anti-rabbit antibody and subsequently stained with anti-keratin 8 antibody (35βH11) (5) and detected with rhodamine-conjugated goat anti-mouse antibody. Bar = 4 μm.

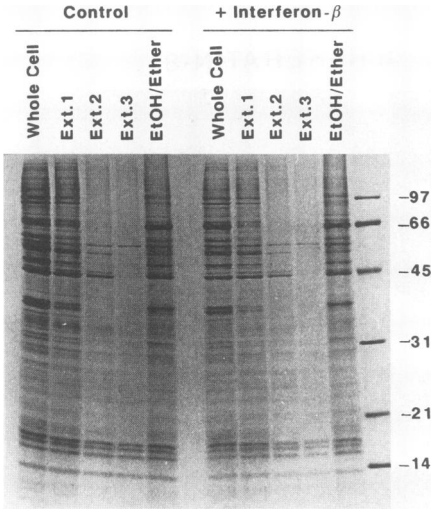

FIG. 7. SDS-PAGE analysis of extracted A549 cells. Subconfluent cultures of A549 cells were grown on coverslips and incubated for 24 h in the absence (Control) or presence (+ Interferon-β) of 1,000 IU of IFN-β per ml. Cells attached to coverslips were solubilized directly into SDS sample buffer (Whole Cell), extracted as described in Material and Methods (11) with 0.5% Triton X-100 and 4 M glycerol for 3 min at 37°C (Ext.1), 0.5% Triton X-100 for 30 min at 37°C (Ext.2), or 0.5% Triton X-100 for 30 min at 37°C and then 0.3 M KI at 4°C (Ext.3), or subjected to successive incubations in 70% EtOH, 50% EtOH–50% ether, 50% EtOH, and H_2O (EtOH/Ether) (42) followed by solubilization in SDS sample buffer. Samples were resolved by SDS-PAGE (12% gel) and stained for total protein with Coomassie blue. Positions of molecular weight markers are indicated in kilodaltons on the right.

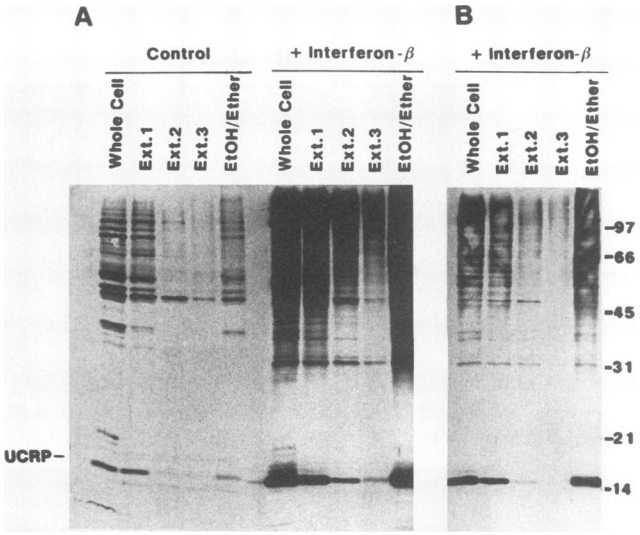

FIG. 8. Immunoblot analysis of extracted A549 cells. Parallel samples from A549 cell extracts as described in the legend to Fig. 7 were resolved by SDS-PAGE, transferred to nitrocellulose, and probed with anti-UCRP antibodies. Immunorecognition was detected by autoradiography following incubation with ^{125}I-protein A. Panel B represents a fivefold-shorter exposure of panel A.

(Fig. 8A, Whole Cell + Interferon-β). The autoradiogram of Fig. 8A reflects the relative increases in the free and conjugated UCRP pools in response to IFN-β induction; however, the marked induction of UCRP adducts obscures details of the resulting molecular weight distribution. Figure 8B shows the autoradiographic pattern of the interferon-induced blot of Fig. 8A exposed for one-fifth the time to normalize for the relative induction in total UCRP protein derived from direct quantitation. The normalized exposure of Fig. 8B reveals that the distribution of UCRP conjugates induced in response to IFN-β is qualitatively similar to that of uninduced cells in containing bands of identical mobility; however, the relative abundance of the various bands is altered during interferon induction. This suggests a change in relative specificity for UCRP conjugation in response to interferon induction.

Figure 8 demonstrates that extraction 2 eliminates most of the free and conjugated UCRP from uninduced control cells, as expected since UCRP is a soluble cytosolic protein (6, 16, 19). In interferon-treated cells, a considerable fraction of free and conjugated UCRP is retained in extract 2 and persists even after extraction 3 (Fig. 8A, + Interferon-β). Since the majority of intracellular proteins are removed by extraction 2, as judged from Coomassie blue staining (Fig. 7), retention of significant free and conjugated UCRP in the final two extraction samples suggests these proteins bind to intermediate filaments, the dominant proteins retained after extraction 3. This binding must be relatively specific, since the free and conjugated forms of UCRP, present in low abundance compared with total protein, are observed following extraction 3 (Fig. 8, + Interferon-β, Ext.3) while little total protein is retained (Fig. 7). No effort was made to estimate the fraction of total UCRP originally bound to the intermediate filaments, since the results of Fig. 8 indicate that the conditions of extractions 2 and 3 progressively remove these adducts. Work is currently in progress to confirm directly that free and conjugated UCRP bind to intermediate filaments.

The results of Figure 8 indicate that the intermediate filament-associated UCRP signal detected immunocytochemically in uninduced A549 cells principally originates from conjugated rather than free polypeptide. Moreover, the majority of the signal is derived from an intermediate filament-associated UCRP conjugate of 48 kDa, representing a target protein of approximately 33 kDa when the molecular mass contribution from UCRP (15 kDa) is subtracted. Three observations preclude the 48-kDa UCRP conjugate arising as an artifact from cross-reaction of the anti-UCRP antibody with cytokeratin 18, which has a similar relative molecular mass (not shown). The 48-kDa UCRP conjugate migrated slightly above the band of cytokeratin 18 when immunoblots such as that in Fig. 8 were counterstained for protein. In addition, on parallel immunoblots, monoclonal antibody CK-5 detected cytokeratin 18 but not the 48-kDa band bound by the anti-UCRP antibodies. Finally, anti-UCRP failed to detect a recombinant human cytokeratin 18 standard present on a control immunoblot at approximately the same amount as that contained in an extract 3 sample such as that in Fig. 8.

DISCUSSION

The biological response of UCRP intracellularly is assumed to require its covalent ligation to specific target proteins (6, 19). As an approach to identifying substrate targets for UCRP conjugation and therefore to define a potential function(s) for this posttranslational modification, immunocytochemical studies were initiated to determine the intracellular distribution of these adducts. A significant fraction of the immunocytochemical signal detected with affinity-purified anti-UCRP polyclonal probes distributes in a punctate filamentous pattern under low magnification (Fig. 1 and 2). Treatment with IFN-β induced the synthesis of UCRP and a corresponding increase in the

diffuse cytoplasmic distribution in A549 cells. However, the filamentous distribution of UCRP remained detectable within the diffuse staining of soluble free and conjugated UCRP (Fig. 2), consistent with previous findings that the target protein population susceptible to UCRP conjugation is largely conserved between uninduced and interferon-treated cells (19). Additional studies demonstrated that the distribution of UCRP colocalized with the keratin network in A549 cells (Fig. 6), vimentin filaments in both A549 and MG-63 cells (not shown), and keratin in primary kerotinocytes (not shown), indicating that UCRP associates with several types of intermediate filament proteins. The punctate distribution of UCRP was not uniform along the intermediate filaments. Regions of the fibers devoid of associated UCRP were randomly distributed in the cell. It is unlikely that the regions devoid of associated UCRP resulted from the fixation procedures, since several protocols resulted in a similar distribution. It is possible that the seemingly undecorated regions contain low levels of associated UCRP below the limit of detection by immunofluorescence. Alternatively, the equilibrium position for binding of UCRP conjugates to the fibers may be freely reversible for the intracellular concentrations of these adducts so that the irregular distribution reflects transient fluctuations in distribution that are trapped during fixation.

Previous work by Fried and coworkers has suggested that free ubiquitin associates with intermediate filaments (4) and microtubules (29). In addition, ubiquitin conjugates have been identified in inclusion bodies of several degenerative diseases, including Alzheimer's dementia (24, 25, 45), Parkinson's disease (24), and amyotrophic lateral sclerosis (26, 27). In the present studies, the cytoskeletal distribution of UCRP differs significantly from that of ubiquitin, which exhibits a diffuse cytoplasmic localization and prominent nuclear staining (Fig. 1C). We consistently failed to observe a cytoskeletal distribution for ubiquitin when affinity-purified rabbit polyclonal antibodies against this polypeptide were used. The competition experiments of Fig. 1 rule out cross-reaction between anti-ubiquitin and anti-UCRP antibodies in immunocytochemical applications; therefore, it is possible that the discrepancy between our inability to detect ubiquitin localization to the cytoskeleton and the reports of Fried et al. reflects cross-reaction of their monoclonal probes with endogenous UCRP. Alternatively, the data do not rule out the possibility that the cytoskeletal distribution of ubiquitin is not a general feature of all cells, unlike that of UCRP. More recently, Lowe and coworkers have found that the distribution of UCRP in several pathological and normal human tissues, including those showing ubiquitin localization to inclusion bodies, is distinct from that of ubiquitin (21). These findings emphasize the importance of assessing potential cross-reaction between immunoprobes prepared against the two polypeptides when interpreting results from localization studies.

Rigorous extraction with nonionic detergent and 0.3 M KI (extraction 3) demonstrated that the cytoskeletal pattern for UCRP resulted from colocalization with intermediate filaments (Fig. 6C). Since the affinity-purified anti-UCRP antibodies do not discriminate between free and conjugated polypeptide, the parallel Western blot of Fig. 8 was critical in distinguishing between these two pools in their binding to intermediate filaments. The autoradiogram of Fig. 8A shows that the cytoskeletal distribution of UCRP in uninduced cells following extraction 3 (Fig. 6G) derives principally from conjugated rather than free UCRP. Most of the cytoskeletal UCRP signal is attributable to a single adduct of 48 kDa, although a number of higher-molecular-mass conjugates are present at lower levels. The UCRP conjugates must be partially sensitive to the conditions of extraction 3, since the autoradiographic intensity of the 48-kDa adduct is about 25% of that following extraction 2, which itself is nearly quantitatively retained compared to that for the whole cell extract (Fig. 8A, Control). In contrast, the marked accumulation of free and conjugated UCRP pools following 24 h of interferon induction is accompanied by a proportional increase in the retention of both populations following extraction 3 (Fig. 8A, + Interferon-β). The latter result is not a consequence of incomplete extraction, since the distributions of proteins retained following extraction 3 are comparable between control and interferon-induced cultures when detected by Coomassie blue staining (Fig. 7). However, as found with the uninduced cells, both populations of UCRP are subject to some loss during the conditions of extraction 3, since the 48-kDa conjugate band is reduced approximately fourfold from that present following extraction 2 (Fig. 8A, + Interferon-β). This loss is particularly evident in Fig. 8B, for which the Western was exposed for a proportionately shorter time to correct for the increase in total UCRP present within the cells. The distribution of UCRP conjugates in Fig. 8B is somewhat different from that of uninduced cells (Fig. 8A), which may reflect subtle changes in the target protein specificity for conjugation during interferon induction.

The results of Fig. 8 suggest that the cytoskeletal distribution of UCRP is due to the noncovalent adsorption of the polypeptide (free or conjugated) to the intermediate filament network, for which UCRP may serve as a transposable *trans*-acting binding factor for directing the association of otherwise soluble target proteins to these fibers. We believe this putative binding to be specific relative to total protein, since a qualitatively greater fraction of total UCRP (Fig. 8) than of total protein (Fig. 7) is retained following the conditions of extraction 3. It is evident from Fig. 8 that the successive extraction steps strip UCRP from the intermediate filaments; therefore, we have made no attempt to quantitate the fraction of UCRP bound to these fibers prior to extraction. There is precedence for binding of interferon-induced proteins to the cytoskeleton. The interferon-induced MxA protein, which inhibits replication of influenza virus in cultured mouse cells, has been shown to bind transiently to cytoskeletal proteins (12). In contrast, many viral proteins also associate with the intermediate filament network presumably as sites for the assembly of new viral particles, such as demonstrated by frog virus 3 (28). Other viral infections induce morphological changes in the cytoskeleton, such as the altered distribution of vimentin intermediate filaments following cleavage of these structural proteins by human immunodeficiency virus type 1 protease (36). Moloney mouse sarcoma virus specifically modifies vimentin by phosphorylation, which may modulate the function of vimentin filaments in transformed cells (37). The association of UCRP conjugates with these filaments could potentially either block binding or inhibit the action of such viral proteins as part of the antiviral activity of the polypeptide.

Low constitutive levels of conjugated and free UCRP have been observed previously in various cell lines (6, 19) and human tissues (19–21). The results of Fig. 3 confirm that the low basal level of UCRP is not a consequence of autoinduction by endogenous interferon secretion, since both free and conjugated UCRP are found by immunoblot analysis in confluent A549 cells passaged three times in the presence of sufficient anti-IFN-α and anti-IFN-β antibodies to neutralize $>10^2$ IU of the cytokines per ml. Several other interferon-induced proteins are found at low constitutive levels in the absence of interferon treatment (1, 17), indicating that some of the mechanisms for interferon action are mediated by upregulating preexisting

pathways involved in basal metabolism. By inference, it is likely that UCRP also serves a basal regulatory function which is recruited during the interferon response. Other intermediate filament-associated proteins have been found to distribute in a punctate pattern similar to that observed here for UCRP (18) and to serve in bridging filaments (43). Therefore, the potential exists that UCRP or its conjugates contribute to the organization of the cytoskeletal network.

Our current understanding of the UCRP conjugation pathway is not adequate to ascribe a defined function for UCRP adduct formation. As a ubiquitin homolog, UCRP conjugation may target a separate set of proteins for degradation via the ATP-ubiquitin-dependent degradative pathway (40). If this is the case, then association of UCRP conjugates with intermediate filaments may contribute to the regulation, disassembly, and degradation of these fibers during cellular differentiation and division. Since UCRP is one of the first proteins induced following interferon treatment, it is likely that this protein serves a fundamental role in the interferon response, for which its ligation to intracellular targets and their subsequent association with intermediate filaments represents a novel mechanism for this transduction pathway.

ACKNOWLEDGMENTS

This work was supported in part by Public Health Service grant GM47426 (A.L.H.) and a predoctoral fellowship from the American Heart Association—Wisconsin Affiliate (K.R.L.). K.R.L. is a fellow of the Medical College of Wisconsin Medical Scientist Training Program.

We thank Allen Gown for helpful discussions and for supplying monoclonal antibodies 35βH11 and 43βE8 and Triton Bioscience for supplying human IFN-β_{ser}. We also thank George Giudice and Frank Soloman for helpful advice and Werner Franke and Ilse Hofmann for supplying a sample of human recombinant keratin 18.

REFERENCES

1. **De Maeyer, E., and J. De Maeyer-Guignard.** 1988. Interferon and other regulatory cytokines. Wiley, New York.
2. **Fairley, J. A., G. A. Scott, K. D. Jensen, L. A. Goldsmith, and L. A. Diaz.** 1991. Characterization of keratocalmin, a calmodulin-binding protein from human epidermis. J. Clin. Invest. **88:**315–322.
3. **Farrell, P. J., R. J. Broeze, and P. Lengyel.** 1979. Accumulation of an mRNA and protein in interferon-treated Ehrlich ascites tumour cells. Nature (London) **279:**523–525.
4. **Fried, V. A., and H. T. Smith.** 1989. Ubiquitin: a multifunctional regulatory protein associated with the cytoskeleton. Prog. Clin. Biol. Res. **317:**733–744.
5. **Gown, A. M., and A. M. Vogel.** 1982. Monoclonal antibodies to intermediate filament proteins of human cells: unique and cross-reacting antibodies. J. Cell Biol. **95:**414–424.
6. **Haas, A. L., P. Ahrens, P. M. Bright, and H. Ankel.** 1987. Interferon induces a 15-kilodalton protein exhibiting marked homology to ubiquitin. J. Biol. Chem. **262:**11315–11323.
7. **Haas, A. L., and P. M. Bright.** 1985. The immunochemical detection and quantitation of intracellular ubiquitin-protein conjugates. J. Biol. Chem. **260:**12464–12473.
8. **Harlow, E., and D. Lane.** 1988. Antibodies, a laboratory manual. Cold Spring Harbor Laboratory Press, Cold Spring Harbor, N.Y.
9. **Hershko, A., and A. Ciechanover.** 1992. The ubiquitin system for protein degradation. Annu. Rev. Biochem. **61:**761–807.
10. **Hershko, A., A. Ciechanover, H. Heller, A. L. Haas, and I. A. Rose.** 1980. Proposed role of ATP in protein breakdown: conjugation of protein with multiple chains of the polypeptide of ATP-dependent proteolysis. Proc. Natl. Acad. Sci. USA **77:**1783–1786.
11. **Heuser, J. E., and M. W. Kirschner.** 1980. Filament organization revealed in platinum replicas of freeze-dried cytoskeletons. J. Cell Biol. **86:**212–234.
12. **Horisberger, M. A.** 1992. Interferon-induced human protein MxA is a GTPase which binds transiently to cellular proteins. J. Virol. **66:**4705–4709.
13. **Johnson, G. D., R. S. Davidson, K. C. McNamee, G. Russell, D. Goodwin, and E. J. Holborow.** 1982. Fading of immunofluorescence during microscopy: a study of the phenomenon and its remedy. J. Immunol. Methods **55:**231–242.
14. **Jonnalagadda, S., T. R. Butt, J. Marsh, E. J. Sternberg, C. K. Mirabelli, D. J. Ecker, and S. T. Crooke.** 1987. Expression and accurate processing of yeast penta-ubiquitin in Escherichia coli. J. Biol. Chem. **262:**17750–17756.
15. **Knight, E., Jr., D. Fahey, B. Cordova, M. Hillman, R. Kutny, N. Reich, and D. Blomstrom.** 1988. A 15-kDa interferon-induced protein is derived by COOH-terminal processing of a 17-kDa precursor. J. Biol. Chem. **263:**4520–4522.
16. **Korant, B. D., D. C. Blomstrom, G. J. Jonak, and E. Knight, Jr.** 1984. Interferon-induced proteins. Purification and characterization of a 15,000-dalton protein from human and bovine cells induced by interferon. J. Biol. Chem. **259:**14835–14839.
17. **Koromilas, A. E., S. Roy, G. N. Barber, M. G. Katze, and N. Sonenberg.** 1992. Malignant transformation by a mutant of the IFN-inducible dsRNA-dependent protein kinase. Science **257:**1685–1689.
18. **Lawson, D.** 1983. Epinemin: a new protein associated with vimentin filaments in non-neural cells. J. Cell Biol. **97:**1891–1905.
19. **Loeb, K. R., and A. L. Haas.** 1992. The interferon-inducible 15-kDa ubiquitin homolog conjugates to intracellular proteins. J. Biol. Chem. **267:**7806–7813.
20. **Loeb, K. R., and A. L. Haas.** 1993. Ph.D. thesis. (publication no. 9411869). Medical College of Wisconsin, Milwaukee.
21. **Lowe, J., H. McDermott, K. R. Loeb, M. Landon, A. L. Haas, and R. J. Mayer.** Immunohistochemical localisation of ubiquitin cross-reactive protein in human tissues. Submitted for publication.
22. **Manetto, V., G. Perry, M. Tabaton, P. Mulvihill, V. A. Fried, H. T. Smith, P. Gambetti, and L. Autilio-Gambetti.** 1988. Ubiquitin is associated with abnormal cytoplasmic filaments characteristic of neurodegenerative diseases. Proc. Natl. Acad. Sci. USA **85:**4501–4505.
23. **Matthes, T., A. Wolff, P. Soubiran, F. Gros, and G. Dighiero.** 1988. Antitubulin antibodies. II. Natural autoantibodies and induced antibodies recognize different epitopes on the tubulin molecule. J. Immunol. **141:**3135–3141.
24. **Mayer, R. J., J. Arnold, L. Laszlo, M. Landon, and J. Lowe.** 1991. Ubiquitin in health and disease. Biochim. Biophys. Acta **1089:**141–157.
25. **Mori, H., J. Kondo, and Y. Ihara.** 1987. Ubiquitin is a component of paired helical filaments in Alzheimer's disease. Science **235:**1641–1644.
26. **Murayama, S., H. Mori, Y. Ihara, T. W. Bouldin, K. Suzuki, and M. Tomonaga.** 1990. Immunocytochemical and ultrastructural studies of lower motor neurons in amyotrophic lateral sclerosis. Ann. Neurol. **27:**137–148.
27. **Murayama, S., Y. Ookawa, H. Mori, I. Nakano, Y. Ihara, S. Kuzuhara, and M. Tomonaga.** 1989. Immunocytochemical and ultrastructural study of Lewy body-like hyaline inclusions in familial amyotrophic lateral sclerosis. Acta Neuropathol. **78:**143–152.
28. **Murti, K. G., R. Goorha, and M. W. Klymkowsky.** 1988. A functional role for intermediate filaments in the formation of frog virus 3 assembly sites. Virology **162:**264–269.
29. **Murti, K. G., H. T. Smith, and V. A. Fried.** 1988. Ubiquitin is a component of the microtubule network. Proc. Natl. Acad. Sci. USA **85:**3019–3023.
30. **Ohta, M., N. Marceau, G. Perry, V. Manetto, P. Gambetti, L. Autilio-Gambetti, J. Metuzals, H. Kawahara, M. Cadrin, and S. W. French.** 1988. Ubiquitin is present on the cytokeratin intermediate filaments and Mallory bodies of hepatocytes. Lab. Invest. **59:**848–856.
31. **Ozkaynak, E., D. Finley, M. J. Solomon, and A. Varshavsky.** 1987. The yeast ubiquitin genes: a family of natural gene fusions. EMBO J. **6:**1429–1439.
32. **Reich, N., B. Evans, D. Levy, D. Fahey, E. Knight, Jr., and J. E. Darnell, Jr.** 1987. Interferon-induced transcription of a gene encoding a 15-kDa protein depends on an upstream enhancer element. Proc. Natl. Acad. Sci. USA **84:**6394–6398.
33. **Riley, D. A., J. L. W. Bain, S. Ellis, and A. L. Haas.** 1988. The quantitation and immunohistochemical localization of ubiquitin

conjugates within rat red and white skeletal muscles. J. Histochem. Cytochem. **36**:621–632.
34. **Schlesinger, D. H., G. Goldstein, and H. D. Niall.** 1975. The complete amino acid sequence of ubiquitin, an adenylate cyclase stimulating polypeptide probably universal in living cells. Biochemistry **14**:2214–2218.
35. **Sen, G. C., and P. Lengyel.** 1992. The interferon system. A bird's eye view of its biochemistry. J. Biol. Chem. **267**:5017–5020.
36. **Shoeman, R. L., B. Honer, T. J. Stoller, C. Kesselmeier, M. C. Miedel, P. Traub, and M. C. Graves.** 1990. Human immunodeficiency virus type 1 protease cleaves the intermediate filament proteins vimentin, desmin, and glial fibrillary acidic protein. Proc. Nat. Acad. Sci. USA **87**:6336–6340.
37. **Singh, B., and R. B. Arlinghaus.** 1989. Vimentin phosphorylation by p37mos protein kinase in vitro and generation of a 50-kDa cleavage product in v-mos-transformed cells. Virology **173**:144–156.
38. **Small, J. V., S. Zobeley, G. Rinnerthaler, and H. Faulstich.** 1988. Coumarin-phalloidin: a new actin probe permitting triple immunofluorescence microscopy of the cytoskeleton. J. Cell Sci. **89**:21–24.
39. **Tolle, H. G., K. Weber, and M. Osborn.** 1986. Microinjection of monoclonal antibodies to vimentin, desmin, and GFA in cells which contain more than one IF type. Exp. Cell Res. **162**:462–474.
40. **Varshavsky, A.** 1992. The N-end rule. Cell **69**:725–735.
41. **Vijay-Kumar, S., C. E. Bugg, and W. J. Cook.** 1987. Structure of ubiquitin refined at 1.8 A resolution. J. Mol. Biol. **194**:531–544.
42. **von der Mark, K., V. Gauss, H. von der Mark, and P. Muller.** 1977. Relationship between cell shape and type of collagen synthesised as chondrocytes lose their cartilage phenotype in culture. Nature (London) **267**:531–532.
43. **Wang, E., J. G. Cairncross, W. K. Yung, E. A. Garber, and R. K. Liem.** 1983. An intermediate filament-associated protein, p50, recognized by monoclonal antibodies. J. Cell. Biol. **97**:1507–1514.
44. **Wilkinson, K. D., and T. K. Audhya.** 1981. Stimulation of ATP-dependent proteolysis requires ubiquitin with the COOH-terminal sequence Arg-Gly-Gly. J. Biol. Chem. **256**:9235–9241.
45. **Yamaguchi, H., Y. Nakazato, T. Kawarabayashi, K. Ishiguro, Y. Ihara, M. Morimatsu, and S. Hirai.** 1991. Extracellular neurofibrillary tangles associated with degenerating neurites and neuropil threads in Alzheimer-type dementia. Acta Neuropathol. **81**:603–609.